A study of the autofluorescence of parylene materials for μTAS applications

Bo Lu,*[a] Siyang Zheng,[b] Brandon Quoc Quach[a] and Yu-Chong Tai[a]

Received 27th November 2009, Accepted 19th March 2010
First published as an Advance Article on the web 29th April 2010
DOI: 10.1039/b924855b

Parylene-C has been widely used as a biocompatible material for microfluidics and micro total analysis system (μTAS) applications in recent decades. However, its autofluorescence can be a major obstacle for parylene-C based devices used in applications requiring sensitive fluorescence detection. In this paper, Parylene-C was compared with other commonly used polymer and plastic materials in μTAS devices for their autofluorescence. We also report here an in-depth study of the behaviors and mechanisms of the autofluorescence of parylene-C, as well as several other commercialized members in the parylene family, including parylene-D, parylene-N and parylene-HT, using epifluorescence microscopy, fluorimeter and infrared spectroscopy. Strong autofluorescence was induced in parylene-C during short-wavelength excitation (*i.e.* UV excitation). Variation of autofluorescence intensity of parylene-C film was found to be related to both dehydrogenation and photo-oxidation. Moreover, the influence of microfabrication process on parylene-C autofluorescence was also evaluated. Parylene-HT, which exhibits low initial autofluorescence, decreasing autofluorescence behavior under UV excitation and higher UV stability, can be a promising alternative for μTAS applications with fluorescence detection.

Introduction

Polymers and plastics are playing an increasingly important role in the microfluidics and μTAS field.[1,2] Compared to the devices adopting traditional materials like glass, quartz or silicon, relatively inexpensive and disposable devices could be made with polymers and plastics.[1] Depending on different applications, the bulk, surface or interface properties of those materials can greatly affect the device performance. For instance, for a large number of biomedical applications, on-chip fluorescence detection has been the golden standard. Many of them require precise detection of small fluorescence signals due to the small sample volume and low concentration of fluorophores.[3–5] In these cases, autofluorescence of the chip material itself becomes important, since it may interfere or even overwhelm the signals of interest. However, it is well known that many polymers and plastics are fluorescent when excited by UV or even visible light.[6,7]

Parylene is a tradename for a group of poly(p-xylylene) polymers (Fig. 1). It is gaining more and more attention for microfluidics and μTAS applications.[8–11] Parylene-C is the most commonly used material in the parylene family. As a biocompatible polymer with the highest USP (U.S. Pharmacopeia) class VI approval, parylene-C has found numerous applications for biomedical implantation. This mechanically strong and flexible material has a Young's modulus of 4 GPa and high malleability that can withstand up to 200% elongation. Its high chemical resistance is also desirable as a microfluidics and μTAS chip material. Unfortunately, the undesired autofluorescence of parylene-C sometimes can be a major obstacle for its use in devices with fluorescence detection, especially for those that require ultraviolet (UV) light excitation. For instance, the strong autofluorescence in our previously reported parylene-C microfilters prevented us from using common chemical dyes, such as DAPI (4′,6-diamidino-2-phenylindole) (excitation maximum (ex): 358 nm; emission maximum (em): 461 nm) or Hoechst 33342 (ex: 350 nm; em: 461 nm), and fluorophore (especially blue) conjugated antibodies for circulating tumor cell (CTC) enumeration after on-chip enrichment from patient blood samples (Fig. 2).[12] Strong blue autofluorescence was also found in parylene-C probe for neural prosthesis application, when observing Hoechst stained neural stem cells.[13] Although the autofluorescence influence is less severe when detecting long wavelength fluorescence signals (*e.g.* green or red),[14,15] it may still disturb the detection if the target fluorescence signal itself is very small, such as on-chip real-time PCR or on-chip flow cytometer applications.[5]

Only a few reports have been devoted to parylene fluorescence study.[16–19] Kochi *et al.*[16] studied the emission spectrum of as-deposited parylene-N film and found an emission peak at 370 nm, which was similar to the emission spectrum of *trans*-stilbene. The initial autofluorescence of parylene-N film was attributed to the small amount of C=C unsaturation in the main chain induced during the pyrolytic production of parylene film.[16] No attention was paid, however, to the fluorescence behavior during continuous UV illumination or the possible expansion of the spectra into the visible range. It has been reported that fluorescent sites could be created in parylene-C and parylene-D film by 280 nm UV illumination,[17] or by exposure to active argon or helium plasma.[18] However, the possible mechanisms of the induced fluorescence and the fluorescence behavior during continuous UV illumination were not discussed. On the other hand, like many other polymers, parylene-C and parylene-N film suffer from degradation under long-time UV radiation due to

[a]*Caltech Micromachining Laboratory, California Institute of Technology, MC 136-93, Pasadena, CA, 91125, USA. E-mail: lubo@mems.caltech.edu*
[b]*Department of Bioengineering, Pennsylvania State University, 224 Hallowell Building, University Park, PA, 16802-6804, USA*

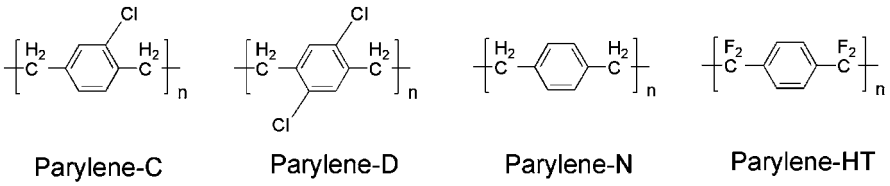

Fig. 1 Structure of parylene-C, parylene-D, parylene-N and parylene-HT films.

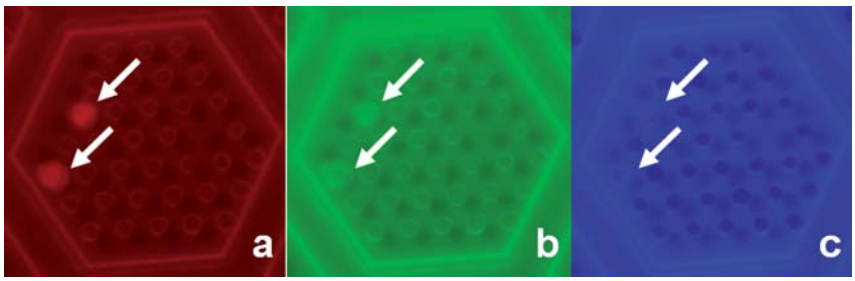

Fig. 2 Strong autofluorescence in parylene-C based dual-layer membrane CTC microfilter. Captured prostate cancer cells were doubly immunofluorescence stained with red and green fluorescence dye conjugated anti-CK (a) and anti-PSA (b). The cell nucleus was stained with DAPI (c). Red and green autofluorescence greatly disturbed the cell detection, while blue autofluorescence totally overwhelmed the stained cells.

UV induced photo-oxidation,[20–24] but no correlation has been studied between this degradation and the variation of fluorescence behavior.

In this work, we report an in-depth study of the fluorescence behaviors and mechanisms of different kinds of parylene films. Parylene-C was compared with other commercially available polymers and plastics for their autofluorescence. Variation of autofluorescence intensity of parylene-C film during continuous UV illumination was found to be related to both dehydrogenation and photo-oxidation. The influence of microfabrication process on parylene-C autofluorescence was also evaluated and discussed. Enhanced autofluorescence during microscope observation, fluorescence detection or the fabrication process makes parylene-C non-ideal for applications where autofluorescence is a concern. Several other commercialized parylene materials, parylene-D, parylene-N and parylene-HT, were also studied. Among them, parylene-HT exhibits low initial autofluorescence with further intensity reduction under UV illumination. Initial autofluorescence of parylene-HT film may come from the residual dimer precursor inside the film, which can be efficiently attenuated to a very low level by intentional UV treatment. Given its much better autofluorescence behavior and high UV stability, parylene-HT can be a useful alternative to parylene-C if low autofluorescence is preferred.

Experimental

Materials

Commercially available parylene dimer precursors DPX-C, DPX-D, DPX-N and parylene-HT (Specialty Coating Systems (SCS)), and diX-C (Daisan Kasei Co., Ltd) were purchased. About 5 μm-thick Parylene films were deposited by a SCS PDS 2035CR parylene coating equipment. In this paper, unless specifically stated, all the parylene films were deposited from SCS dimers. To compare fluorescence properties of parylene with other commonly used polymers and plastics, the following commercial materials were purchased: 1.52 mm poly(methylmethacrylate) sheet (PMMA, McMaster-Carr), 0.38 mm polycarbonate film (PC, McMaster-Carr), 50 μm polyimide film (McMaster-Carr), 13 μm PET polyester film (McMaster-Carr), poly(dimethylsiloxane) (PDMS, Dow Corning Sylgard 184 kit), and 1.14 mm polystyrene tissue culture dish (Becton Dickinson Labware). 0.38 mm PDMS sheets were made by mixing the base to curing agent at a 10 : 1 ratio, degassing, spin coating and baking according to manufacturer's instruction. A 0.98 mm Corning® glass microscope slide (Corning Inc.) was used as an autofluorescence reference.

Observation and recording of fluorescence intensity

Fluorescence was observed under a Nikon E800 epifluorescence microscope (Nikon Inc.). Excitation light came from a USH-102DH 100W mercury arc lamp source (Ushio Inc.), and passed through a dichromatic mirror and one of the following band-pass filters: UV-2E/C, B-2E/C and G-2E/C, with excitation wavelengths of 340–380 nm, 465–495 nm and 528–553 nm, and emission wavelengths of 435–485 nm (blue fluorescence), 515–555 nm (green fluorescence) and 590–650 nm (red fluorescence), respectively. Experiments were done with a 20× objective. Continuous UV illumination was carried out by using UV-2E/C filter. Images were taken with a CCD camera (RT-KE color 3-shot, Diagnostic Instruments). The exposure time referred to the collecting time the CCD camera used to take an image. To avoid saturation of the image, sometimes the exposure time had to be adjusted for different samples. The images were then transferred into 8-bit grayscale images and the fluorescence intensity distributions were calculated using a custom-coded MATLAB (V6.1.0.450, The Mathworks, Inc.) program. In order to evaluate the variations from mercury arc lamp, fluorescence from the Corning® glass microscope slide was used as an internal reference and measured before each experiment and during long-time illumination. Both

UV illumination and fluorescence measurement were performed under atmosphere at room temperature.

Vertical optical alignment during microscope observation may affect the autofluorescence signal observed.[7] For thick samples, autofluorescence intensities may be different when excitation is focused on different vertical positions of the materials.[7] However, for thin films, such as the parylene film we used (5 μm thick), given our exposure and image processing methods, no clear difference was observed when excitation was focused on the surface or into the bulk of the material. In our experiments, excitation was focused on the top surface of the materials.

Fluorescence spectra and infrared spectra

The fluorescence spectra of both parylene film and dimer were measured by a Jobin-Yvon JY3D spectrofluorimeter (HORIBA Jobin Yvon Inc.). To measure the spectra of the dimer, the dimer was dissolved in methanol first and the solution was placed inside a 3-Q-10 quartz fluorometer cuvette (Starna Cells, Inc.). The IR spectra of parylene films were recorded by a Nicolet 6700 FT-IR Spectrometer (Thermo Fisher Scientific Inc.). UV illumination of samples for these spectra experiments were prepared by a UV-Ozone (UVO) instrument (1.12 mW/cm^2, 253.7 nm, Jelight Company, Inc.) in the air environment (Ozone was not used here), which could uniformly produce photo-chemically modified films with large size.

Soaking test

In order to extract the possible fluorescent contaminants and find the mechanism of fluorescence, parylene films were soaked in methanol, toluene and methylene dichloride solvents, accompanied by ultrasonic agitation.

Cell filtration experiment with parylene membrane filters

To show the influence of autofluorescence, both parylene-C and parylene-HT membrane filtration devices for circulating tumor cell (CTC) detection were fabricated by a previously reported process.[4] No autofluorescence pretreatment was performed on the parylene-HT filter. Cultured human prostate cancer cell line LnCaP was used for CTC capture experiments. Cancer cells were spiked into phosphate buffered saline (PBS), and the samples were filtrated using both parylene-C and parylene-HT membrane filters. In order to enumerate the captured cells and observe the nucleus morphology, cells were first fixed in 100% methanol on-filter, and then doubly stained with both Acridine Orange (AO) and DAPI. After staining, filters were extensively washed in PBS to remove the fluorescent dyes remaining on the filter surface.

Results and discussion

Comparison of autofluorescence

Fig. 3a–c show the comparison of initial autofluorescence intensities of 5 μm thick as-deposited parylene-C film with other commonly used commercially available polymers and plastics, including PDMS, PMMA, polycarbonate, polystyrene, polyester and polyimide, measured by the epifluorescence microscope. Since it is reasonable to assume the initial intensity was approximately proportional to the material thickness,[6] the intensities of materials were normalized to 5 μm thickness and also compared in Fig. 3d–f. Among the selected materials, parylene-C has strong initial autofluorescence per unit thickness, although not the worst one. For parylene-C, blue fluorescence intensity was much higher than green or red fluorescence. For applications requiring high sensitivity, extremely small fluorescence signals may be easily buried within this undesired autofluorescence noise.

Autofluorescence behaviors during UV illumination

For many applications involving optical detection or observation, the polymer and plastic microchips will be illuminated for a period of time, thus the trend and variation of autofluorescence under continuous illumination, rather than the initial autofluorescence, are more important. Previous reports showed that a lot of polymers and plastics, including PDMS, PMMA, polycarbonate, polyester and polystyrene had decreasing autofluorescence under continuous illumination, with complex kinetics which are still not fully understood.[6,7] For all four kinds of parylene films studied here, continuous blue or green light illumination under fluorescence microscope did not cause observable green or red autofluorescence intensity variation. Surprisingly, for blue fluorescence under UV excitation, the initial intensity of parylene-C film dramatically increased during a 2 min short-time UV illumination from the microscope light source (Fig. 4a). After UV illumination, green and red fluorescence intensities of the exposed area were also enhanced (Fig. 4b and c). The same phenomena were also found in parylene-C film deposited from diX-C dimer (data not shown). Fig. 5 shows the quantitative measurements of fluorescence variations during short-time UV illumination. Parylene-D film exhibited the same behaviors of enhanced autofluorescence as parylene-C. Autofluorescence intensities of parylene-N film followed the similar trends but only slightly increased. However, parylene-HT film showed a reverse trend with clearly decreasing tendency for blue, green and red fluorescence (Fig. 4d and Fig. 5).

To study the fluorescence mechanism of parylene films, we extended the UV illumination experiments to a long period up to 1000 min and recorded the blue fluorescence intensity variations. Both parylene-C and parylene-D showed a two-stage fluorescence behavior. During initial short-time UV illumination, blue fluorescence increased dramatically (stage 1, Fig. 6a and b insets). However, after reaching its maximum value, the fluorescence intensity started to decay gradually in the following long-time UV illumination (stage 2, Fig. 6a and b). For parylene-N, during the 1000 min illumination, only the increasing stage was observed (Fig. 6c). The long-time illumination of parylene-C, parylene-D and parylene-N were accompanied by a yellow discoloration of the film. Parylene-D had the fastest rate and largest extent of discoloration, while parylene-N had the slowest rate and only slight extent of discoloration even for longer illumination time. Interestingly, although parylene-HT had the largest initial fluorescence intensity, it decreased exponentially from the beginning within a short time upon illumination (Fig. 6d), without any sign of yellow discoloration. Three conclusions can be readily drawn from the analysis: (1) During microscope observation or optical detection where UV light is involved, strong autofluorescence of parylene-C and parylene-D

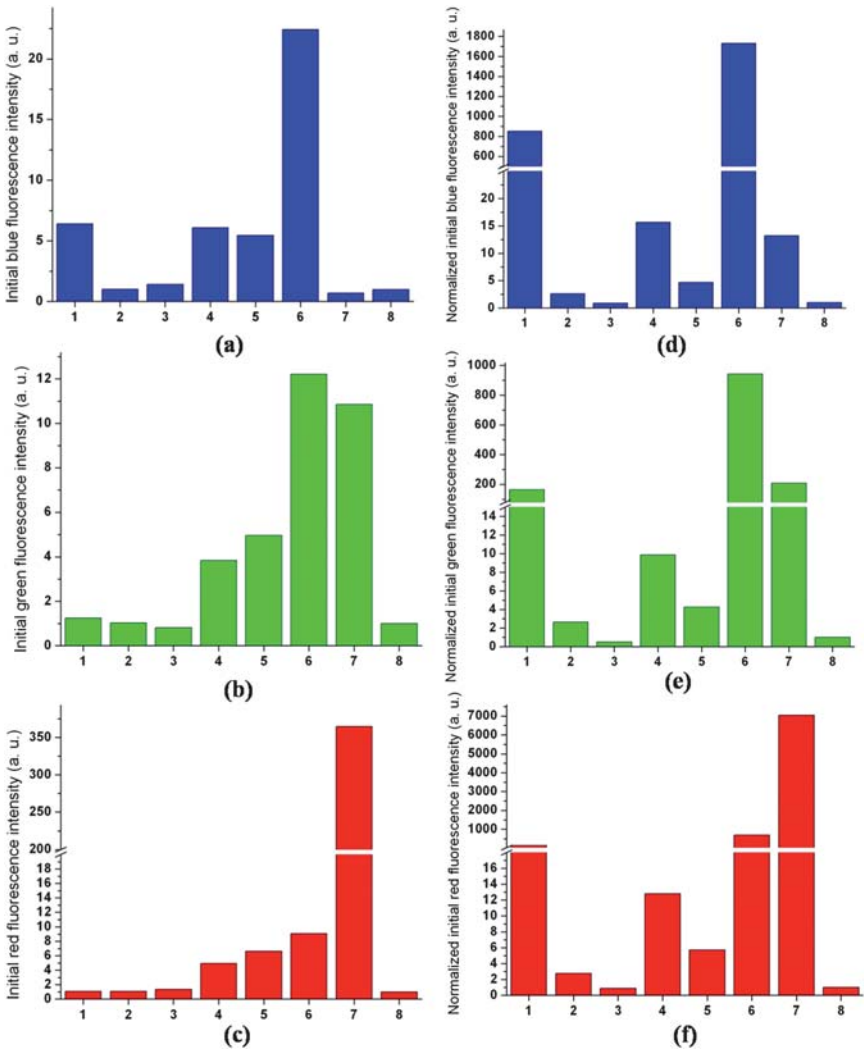

Fig. 3 Comparisons of relative initial autofluorescence intensities of parylene-C with other polymers and plastics. (1): 5 μm parylene-C; (2): 380 μm PDMS; (3): 1.52 mm PMMA; (4): 380 μm polycarbonate; (5): 1.14 mm polystyrene; (6): 12.7 μm polyester; (7): 50.8 μm polyimide; (8): 980 μm Corning® glass slide (control). Autofluorescence of Corning® glass microscope slide was set as 1 (a. u.), and all the other fluorescence intensities were relative to this reference. (a)–(c) show blue, green and red autofluorescence of materials with different thicknesses as purchased or fabricated. (d)–(f) show blue, green and red autofluorescence of materials normalized to 5 μm thickness. All measurements were carried out with a 20× objective. Exposure time: blue (1 s), green (10 s), red (10 s).

can be quickly induced within the first several minutes. Although the increase of parylene-N autofluorescence is much slower, it lasts for a long time. (2) For parylene-C and parylene-D, once the autofluorescence is induced, it takes a long time to reduce the autofluorescence back to the initial level, accompanied by the degradation of films. (3) In contrast, UV illumination can efficiently bleach the autofluorescence of parylene-HT to a very low level within a short time period. Moreover, we observed that the autofluorescence variations of parylene materials were irreversible after the UV illumination was shut down. Discontinuous illumination with time intervals did not change the autofluorescence variation tendency.

Fluorescence mechanism of parylene-C film

Fluorescence spectra of parylene-C film showed that the emission band was red shifted from UV range to visible range during short-time UV illumination, resulting in the enhanced fluorescence in the visible range (Fig. 7). Corresponding infrared (IR) spectra of parylene-C film are shown in Fig. 8. The peaks in the region of 1450∼1610 cm^{-1} could be attributed to C═C double bond stretching vibrations. After 5 min illumination, an increase of the absorption peak around 1560 cm^{-1} occurred, which could be interpreted to the increasing amount of C═C bonds in the chain adjacent to the benzene ring. This change of chemical structure was likely to be a sign of the scission of chain C–H bonds and the occurrence of dehydrogenation. During the long-time UV illumination, however, a reduction of emission band magnitude was observed from fluorescence spectra, with unchanged spectra shape and peak location (Fig. 7). In IR spectra, C═C absorption decreased, while C–O (1100–1300 cm^{-1}) band and C═O (around 1700 cm^{-1}) peak appeared and increased (Fig. 8). This evidence indicated that oxidation happened during long-time illumination.

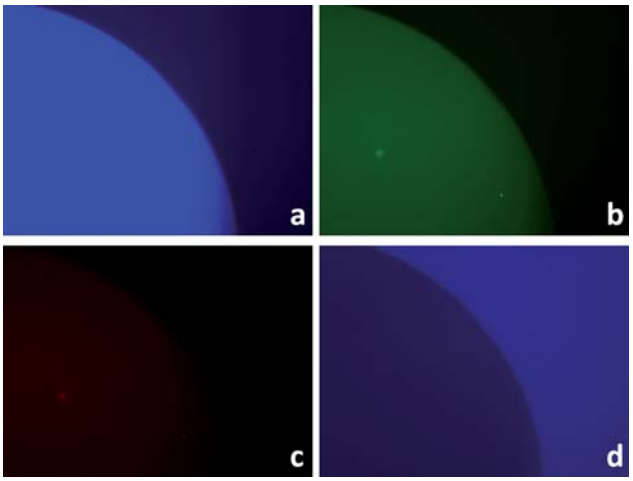

Fig. 4 (a)–(c): Enhanced blue (a), green (b) and red (c) autofluorescence of parylene-C film after 2 min short-time UV illumination. The brighter area was the exposed area under the microscope objective. The darker area was the unexposed area. (d): Reduced blue autofluorescence of parylene-HT film after 2 min short-time UV illumination. The darker area was the exposed area. Images for reduced green or red autofluorescence of parylene-HT were not shown here because the brightness changes were too small for visual discretion. Experiments were carried out with a 20× objective. Exposure time: blue (500 ms), green (10 s), red (10 s).

A few conclusions can be drawn from the above experiment results: (1) fluorescence intensity variations of parylene-C film were related to the variation of unsaturated C=C bonds in the main chain. Analogous to parylene-N, the initial low fluorescence of parylene-C might also come from the small amount of C=C defects in the main chain generated during the deposition process.[16] (2) During short-time UV illumination, dehydrogenation dominated and an increasing amount of C=C bonds formed. This led to an increased conjugation length, which was responsible for the red shift of the fluorescence spectra from the UV range to the visible range.[25] On the other hand, photo-oxidation was limited by oxygen diffusion into the film.[20–24] During the initial illumination, although photo-oxidation also occurred, it was insignificant due to the insufficient contact between oxygen and carbon molecules. (3) During long-time UV illumination, photo-oxidation gradually became dominant. C=C bonds in the main chain were oxidized into C–O or C=O bonds, resulting in the reduction of fluorescence magnitude.

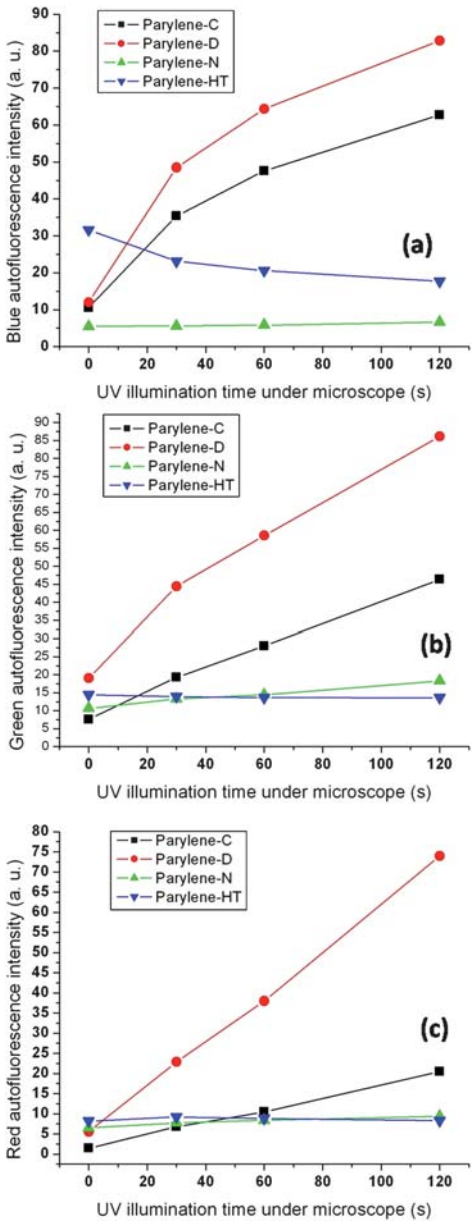

Fig. 5 Quantitative fluorescence intensity variations of parylene films during continuous short-time UV illumination. (a) Blue fluorescence; (b) green fluorescence; (c) red fluorescence. For all kinds of parylene, film thickness was 5 μm. Experiments were carried out with a 20× objective. Exposure time: blue (100 ms), green (10 s), red (10 s).

Fluorescence mechanism of parylene-D and parylene-N films

Here we present a hypothesis to explain the difference in kinetics of fluorescence change in parylene-C, parylene-D and parylene-N. Parylene-D and parylene-N have essentially the same structure with parylene-C, modified only by the number of substitution of chlorine atoms for aromatic hydrogens. Following very similar fluorescence variation trends with both increasing and decreasing stages, parylene-D was likely to have the same fluorescence mechanism with parylene-C. However, up to 1000 min illumination, no decreasing stage was observed for parylene-N, which was probably due to the absence of chlorine substitution. Bera *et al.*[21] found that during the early stage of UV induced photo-oxidation, chloro-related photolytical photoproducts forming at the surface of parylene-C after C–Cl bond scission could prevent the absorption of UV light during subsequent illumination. The formation of these UV-absorbing photoproducts might also be a plausible explanation for the different fluorescence behaviors observed.

During the early stage of UV illumination, dehydrogenation of the chain carbons occurred, accompanied by fluorescence increase. Oxidation at this point started from the surface and was slow since its rate was limited by oxygen diffusion into the parylene film.[23,24] Fluorescence reached its peak when, for parylene-C and parylene-D, the chloro-related photolytical photoproducts

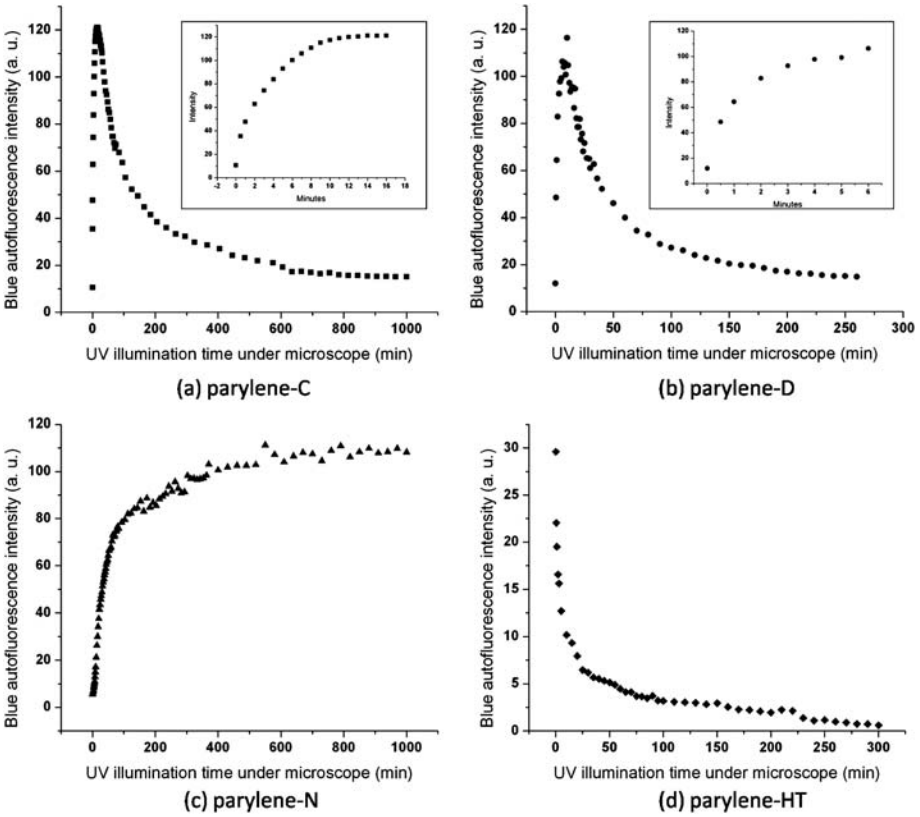

Fig. 6 Quantitative blue fluorescence intensity variations of parylene films during continuous long-time UV illumination. (a) Parylene-C film; (b) parylene-D film; (c) parylene-N film; (d) parylene-HT film. The insets in (a) and (b) show the increasing stage of the curves. For all kinds of parylene, film thickness was 5 μm. Experiments were carried out with a 20× objective. To prevent saturation, exposure time was 100 ms.

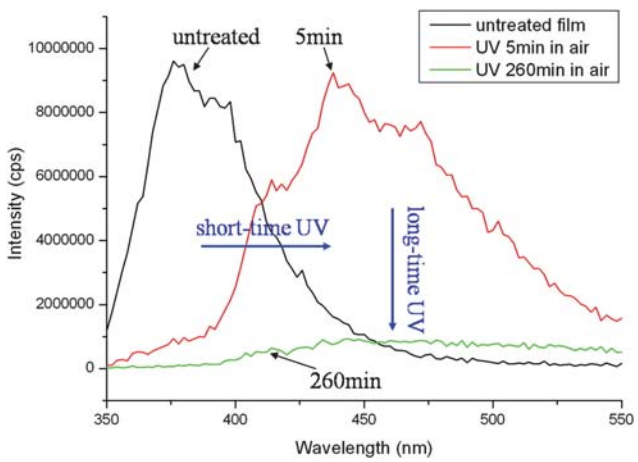

Fig. 7 Fluorescence spectra of parylene-C film, under 280 nm excitation, measured by fluorimeter.

near the surface prevented UV light from penetrating deeper into the film, thus greatly slowing down dehydrogenation as the surface chain hydrogens were consumed. This set the stage for fluorescence to decrease as photo-oxidation, during which the C═C double bonds became oxidized and no longer contributed to fluorescence, began to dominate.

For the non-halogen parylene-N, UV illumination was not accompanied by the formation of UV-absorbing products, thus dehydrogenation was able to continue for a much longer time by accessing hydrogens deeper in the bulk. Photo-oxidation was able to compete, but not yet dominate, during this longer time span, limiting the rate and extent of fluorescence increase. This resulted in a gradually increasing fluorescence curve throughout the 1000 min illumination. The decreasing stage of parylene-N may be expected when illumination time is sufficiently long, the chain hydrogens in the bulk become scarce, further dehydrogenation slows down, and oxidation finally becomes dominant.

Fluorescence mechanism of parylene-HT film

Parylene-HT replaces the chain hydrogen of parylene-N with fluorine. Since the strength of C–F bond is much higher than C–H bond, fluorine extraction is unlikely to occur during UV illumination, which was also verified by fluorescence and IR spectra. No shift of emission band was observed from fluorescence spectra during UV illumination. Reduction of spectra magnitude was in accordance to the decreasing fluorescence intensity. IR spectra of parylene-HT film showed no clear change in the regions of chain C═C bonds, C═O or C–O bonds, indicating the fluorine extraction and photo-oxidation were unlikely to happen under UV illumination (data not shown).

To find the fluorescence mechanism of parylene-HT film, fluorescence spectra of parylene-HT film and its dimer precursor were compared. To measure the spectra of the dimer, we first

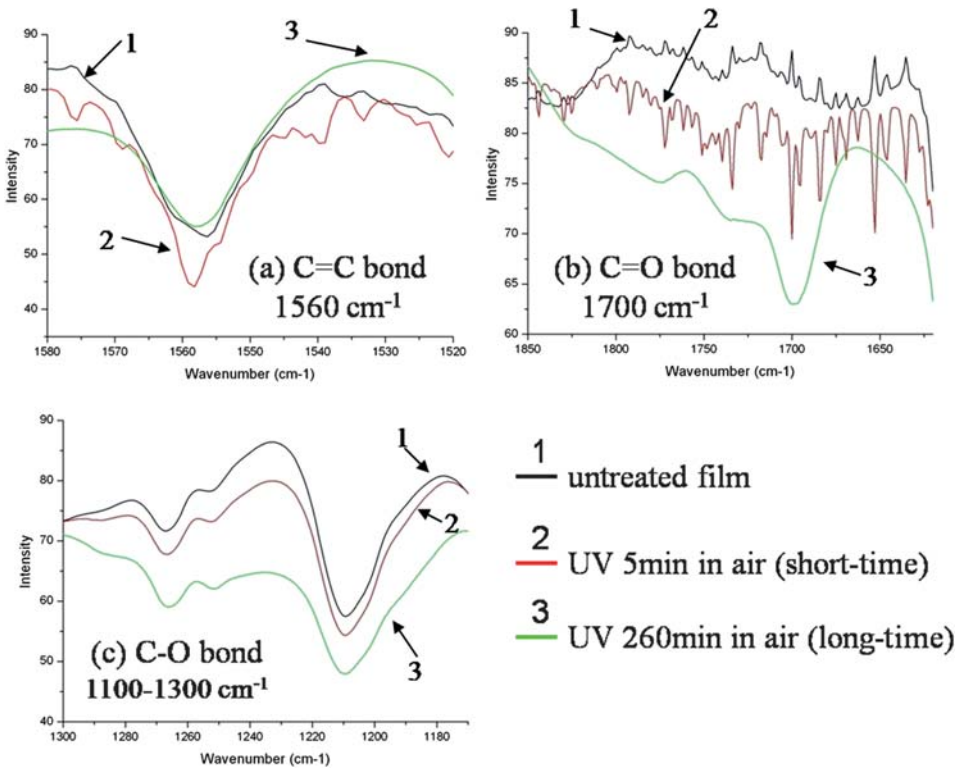

Fig. 8 Infrared spectra of parylene-C film, measured by infrared spectrometer.

scanned the spectra of methanol solvent, then dissolved the dimer in methanol and measured the spectra of the solution. Fig. 9 shows that there were two peaks for the spectra of the solution. When excitation wavelength increased, the peak location of methanol spectra also shifted, while the other peak remained at the same location and only the intensity decreased, which meant the former one was the Raman spectrum of methanol and the latter was the fluorescence spectrum of parylene-HT dimer. A comparison of fluorescence spectra of parylene-HT dimer and film showed the similar peak shape and location, indicating the fluorescence of parylene-HT film might come from the residual dimer inside the film (Fig. 9).

We also verified this conclusion by soaking tests with methanol, toluene and methylene dichloride. Soaking tests with these three solvents had no effects on the fluorescence of parylene-C, parylene-D and parylene-N films. Although methanol or toluene still failed to vary the fluorescence of parylene-HT film, methylene dichloride could effectively reduce the fluorescence intensity of parylene-HT film. After 1.5 h of soaking, the fluorescence intensity was reduced to 35% of its initial level. Therefore,

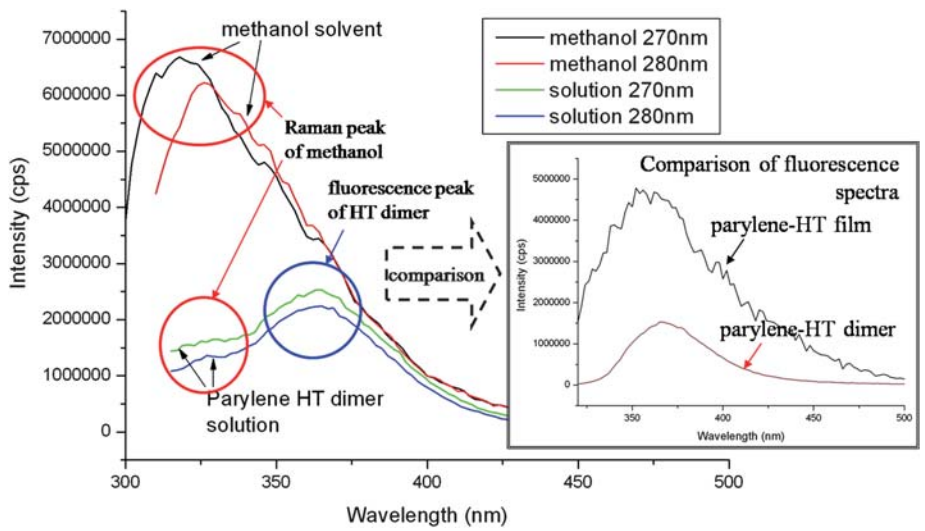

Fig. 9 Fluorescence spectra of parylene-HT dimer and film. Dimer was dissolved in methanol. Inset compares the spectra of parylene-HT dimer and film, which have similar shape and peak location.

methylene dichloride could dissolve and soak out the residual dimer inside the film, resulting in the reduction of fluorescence of the film. One possible explanation of the time-dependent fluorescence intensity reduction of parylene-HT film under UV illumination could be the photobleaching of fluorophores in the dimer. It is also possible that the cleavage of the dimer to its monomeric form happened under UV illumination, resulting in the loss of its fluorescence property.

Autofluorescence problem and possible solutions for parylene based device

Parylene-C is the most popular member in the parylene family and has become the choice of chip material for many applications. However, besides its initial autofluorescence, the undesired autofluorescence of parylene-C based devices can also be easily induced during epifluorescence microscope observation and UV illuminated fluorescence detection. Moreover, it was noticed that for several polymers and plastics, the microchips exhibited higher autofluorescence than the raw materials from which they had been made.[7] Here we compare the autofluorescence of unpatterned parylene-C film with parylene-C based microdevices (Fig. 10). Several μTAS devices, including a real-time PCR chip,[5] a cell culture chamber,[9] a 2D membrane CTC filter,[4] a 3D membrane CTC filter[12] and a 3D splitable membrane CTC filter,[26] were fabricated following different microfabrication processes as described in details in previous publications. In all of those devices, there was parylene-C deposited on low-autofluorescence silicon substrate or parylene-C freestanding structures. The influences of other possible fluorescent materials, such as SU-8 layer, were excluded by observation of the areas without these materials. Fig. 10 shows that in all cases, parylene-C structures in microdevices exhibited considerably higher autofluorescence than unpatterned parylene-C film, after normalized to the same thickness. The additional autofluorescence was likely induced during the microfabrication processes, especially for steps where short-wavelength light sources were used or generated, such as photolithography, plasma etching and metal deposition in e-beam evaporator. Moreover, it was believed that heating parylene film to above certain temperatures could cause the crystalline phase transitions, resulting in the increase of long-wavelength fluorescence.[16] Hence several thermal processes, including vaccum annealing and molten parylene in N_2 environment, were also possibly the suspicious sources of induced strong autofluorescence.

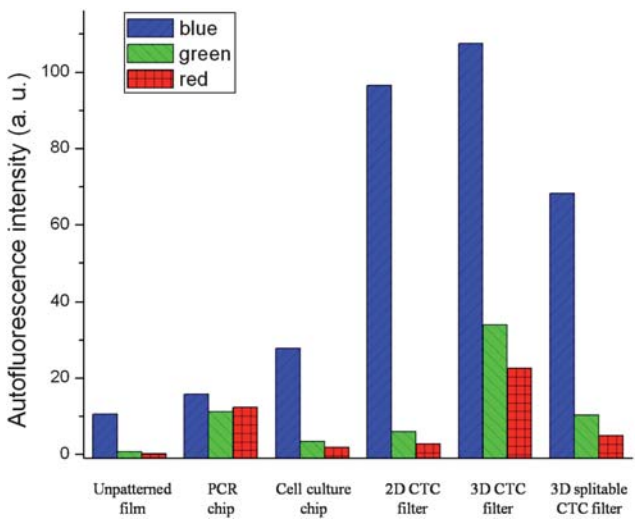

Fig. 10 Comparisons of autofluorescence of unpatterned parylene-C film and parylene-C based devices, including a PCR chip,[5] a cell culture chip,[9] a 2D CTC filter,[4] a 3D CTC filter[12] and a 3D splitable CTC filter.[26] The thickness of all samples was normalized to 5 μm. Experiments were carried out with a 20× objective. Exposure time: blue (100 ms), green (1 s), red (1 s).

Although long-time UV illumination can reduce the autofluorescence, it also degrades the mechanical properties of parylene-C. It was reported that carboxyl groups were produced on parylene-C surface during photo-oxidation process.[21–23] In our experiments, parylene-C film turned yellow and became brittle after long-time UV illumination, losing the advantage of its mechanical properties.

Given this disadvantage, parylene-C may not be the best chip material if sensitive fluorescence detection is required. For these applications, parylene-HT should be considered as an alternative. The fast decreasing autofluorescence profile under UV excitation ensures low fluorescence background during microscope observation and optical detection. Moreover, since parylene-HT has better autofluorescence performance under UV excitation and higher UV stability, the fabrication processes mentioned above did not induce additional autofluorescence in parylene-HT devices. If necessary, intentional UV illumination can be employed as a pretreatment to reduce the initial autofluorescence of parylene-HT devices to a desired level. For instance, it took about 35 min, 140 min and 230 min to reduce the autofluorescence magnitude to 20%, 10% and 5% of its original level, respectively (Fig. 6d). Because of its high UV stability, the mechanical properties of parylene-HT were not influenced after the pretreatment.

Application

As an example illustrating the advantage of the low autofluorescence of parylene-HT, Fig. 11 shows the CTC capture and fluorescence enumeration experiments with parylene-C and parylene-HT based membrane filters. For CTC enumeration, usually antibodies conjugated with red and green fluorophores were used to differentiate captured CTCs and white blood cells. In order to view the cancer cell nucleus morphology, blue fluorescence staining of cell nucleus was also required.[27,28] Previously, autofluorescence of parylene-C led to a bad contrast between stained nucleus and the background or even detection failure.[27] Here we show the improvement of blue fluorescence detection with parylene-HT filter. Cancer cells were doubly stained with both DAPI and AO nucleus dyes. In both cases, green fluorescence from AO staining was only used as a reference, showing the locations of captured cells. For parylene-C device, blue autofluorescence totally overwhelmed the DAPI stained cell nucleus, while the low autofluorescence of parylene-HT device ensured successful detection and observation of the nucleus morphology. In this experiment, no autofluorescence pretreatment was performed on parylene-HT filter, because the DAPI staining was strong. For other applications where the

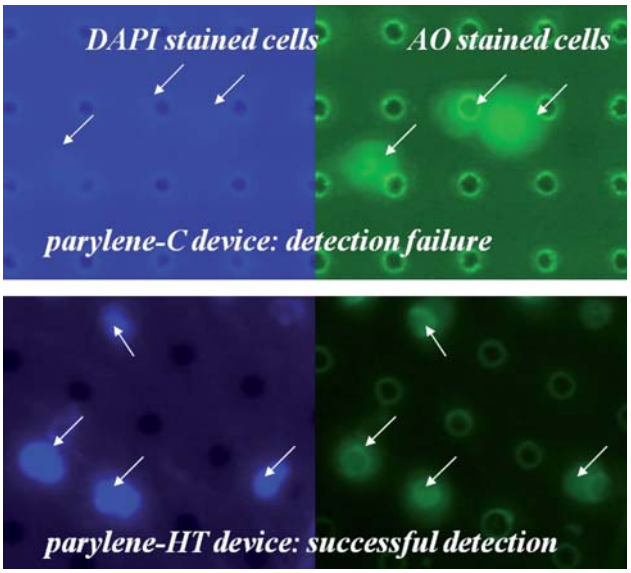

Fig. 11 CTC filtration and enumeration experiments with parylene-C and parylene-HT membrane filters. Captured cancer cells were doubly stained with DAPI and AO. Experiments were carried out with a 20× objective. Exposure time: parylene-C filter (green: 5 s; blue: 30 ms); parylene-HT filter (green: 5 s; blue: 500 ms). Parylene-C device had strong autofluorescence intensity, even with a much shorter exposure time. Parylene-HT device showed low autofluorescence which ensured the successful detection of DAPI stained cells. Green fluorescence with AO staining was only used as a reference to show captured cell locations.

target signal is very weak, pretreatment on parylene-HT device for lower autofluorescence may be necessary.

Conclusion

In this work, a comparison of initial autofluorescence of parylene-C and other commonly used polymers and plastics were studied. For parylene-C, autofluorescence can be easily enhanced during epifluorescence microscope observation, UV illuminated fluorescence detection or microfabrication process. Hence, autofluorescence of parylene-C can become an obstacle for its use in μTAS applications where sensitive fluorescence detection is required. By studying the different dynamics and mechanisms of several materials in the parylene family, including parylene-C, parylene-D, parylene-N and parylene-HT, we showed that parylene-HT, which has better autofluorescence performance, as well as good UV stability, might be a promising alternative chip material if autofluorescence is a concern. The methods and conclusions here are also valuable to the study of other polymers and plastics for μTAS applications.

Acknowledgements

The authors would like to thank Beckman Institute Laser Resource Center of Caltech for the spectrofluorimeter, and Dr John Bercaw's group of Caltech for their FT-IR Spectrometer. The author would like to thank Alec Durrell and Alex Miller for equipment training and experiment assistance. Also the authors would like to thank Kuang Shen from the Chemistry Department of Caltech for his helpful discussion and assistance. The funding is provided by NIH, under Award Number 4000072624.

References

1 H. Becker and C. Gartner, *Anal. Bioanal. Chem.*, 2008, **390**, 89–111.
2 J. West, M. Becker, S. Tombrink and A. Manz, *Anal. Chem.*, 2008, **80**, 4403–4419.
3 Y. S. Shin, K. Cho, S. H. Lim, S. Chung, S. -J. Park, C. Chung, D. -C. Han and J. K. Chang, *J. Micromech. Microeng.*, 2003, **13**, 768–774.
4 S. Zheng, H. K. Lin, J.-Q. Liu, M. Balic, R. Datar, R. J. Cote and Y.-C. Tai, *J. Chromatogr., A*, 2007, **1162**, 154–161.
5 Q. C. Quach and Y. -C. Tai, *Proc. of Hilton Head 2008*, Hilton Head island, SC, USA, 2008, 264–267.
6 K. R. Hawkins and P. Yager, *Lab Chip*, 2003, **3**, 248–252.
7 A. Piruska, I. Nikcevic, S. H. Lee, C. Ahn, W. R. Heineman, P. A. Limbach and C. J. Seliskar, *Lab Chip*, 2005, **5**, 1348–1354.
8 J. Xie, Y. Miao, J. Shih, Y. -C. Tai and T. D. Lee, *Anal. Chem.*, 2005, **77**, 6947–6953.
9 M. C. Liu, D. Ho and Y. -C. Tai, *Sens. Actuators, B*, 2008, **129**, 826–833.
10 P. J. Chen, D. Rodger, R. Agrawal, S. Saati, E. Meng, R. Varma, M. Humayun and Y. -C. Tai, *J. Microelectromech. Syst.*, 2008, **17**, 1342–1351.
11 J. Erickson, A. Tooker, Y. -C. Tai and J. Pine, *J. Neurosci. Methods*, 2008, **175**, 1–16.
12 S. Zheng, H. K. Lin, R. J. Cote and Y. -C. Tai, *Proc. of Hilton Head 2008*, Hilton Head island, SC, USA, 2008, 134–137.
13 E. K. Purcell, J. P. Seymour, S. Yandamuri and D. R. Kipke, *J. Neural Eng.*, 2009, **6**, 026005.
14 J. R. Webster, M. A. Burns, D. T. Burke and C. H. Mastrangelo, *Anal. Chem.*, 2001, **73**, 1622–1626.
15 C. Tung, R. Riehn and R. H. Austin, *Biomicrofluidics*, 2009, **3**, 031101.
16 M. Kochi, K. Oguro and I. Mita, *Eur. Polym. J.*, 1988, **24**, 917–921.
17 W. F. Beach, T. M. Austin and B. J. Humphrey, European Patent Application No. 0 449 291A2, 1991.
18 J. H. Yira and W. F. Beach, U.S. Patent No. 5139813, 1992.
19 Y. Takai and J. H. Calderwood, *Makromol. Chem. Rapid Commun.*, 1980, **1**, 17–21.
20 M. Bera, A. Rivaton, C. Gandon and J. L. Gardette, *Eur. Polym. J.*, 2000, **36**, 1753–1764.
21 M. Bera, A. Rivaton, C. Gandon and J. L. Gardette, *Eur. Polym. J.*, 2000, **36**, 1765–1777.
22 J. B. Fortin and T. -M. Lu, *Thin Solid Films*, 2001, **397**, 223–228.
23 K. G. Pruden, K. Sinclair and S. Beaudoin, *J. Polym. Sci., Part A: Polym. Chem.*, 2003, **41**, 1486–1496.
24 K. G. Pruden and S. P. Beaudoin, *J. Polym. Sci., Part A: Polym. Chem.*, 2004, **42**, 2666–2677.
25 G. Padmanaban and S. Ramakrishnan, *J. Am. Chem. Soc.*, 2000, **122**, 2244–2251.
26 B. Lu, S. Zheng, S. Xie and Y. -C. Tai, *Proc. of μTAS 2009*, Jeju, Korea, 2009, 588–590.
27 H. K. Lin, Ph.D. Thesis, University of Southern California, Los Angeles, CA, USA, 2008.
28 S. Nagrath, L. V. Sequist, S. Maheswaran, D. W. Bell, D. Irimia, L. Ulkus, M. R. Smith, E. L. Kwak, S. Digumarthy, A. Muzikansky, P. Ryan, U. J. Balis, R. G. Tompkins, D. A. Haber and M. Toner, *Nature*, 2007, **450**, 1235–1239.